

Photonic-tunneling experiments

A. Enders and G. Nimtz

II. Physikalisches Institut der Universität zu Köln, Zùlpicher Strasse 77, 5000 Köln 41, Germany

(Received 28 September 1992)

Microwave transmission, in both the frequency and the time domain, through undersized waveguides, which corresponds to potential-barrier tunneling, was studied. The transmission properties inside the potential barriers are shown to be separable from the scattering contributions at the boundaries; no phase shift was found inside. Pulsed measurements in the time domain are used to obtain traversal-time values for opaque barriers. Furthermore, resonant-tunneling experiments through a double-barrier configuration have confirmed that the traversal time and the resonant-state lifetime are different physical entities.

The problem of describing transport properties of waves traveling through a potential barrier still exists. Historically, the mechanisms of wave propagation and its corresponding velocities have been extensively discussed for the dispersive case (phase, group, energy, signal, and forerunner velocities).¹ However, the transport properties of solutions of the Helmholtz wave equation with a purely imaginary eigenvalue for the wave vector k are still not understood. Such eigenvalues have no oscillations in space, and therefore, cannot be regarded as propagating waves. Such solutions occur, e.g., in the case of undersized waveguides, for electromagnetic fields and are often called evanescent modes. The eigenvalue equation for the lowest, so-called H_{10} mode of a rectangular waveguide with cross section $a \times b$ with $a < b$ is given by (c being the velocity of light in vacuum)²

$$k^2 = \left[\frac{2\pi}{\lambda_{\text{vac}}} \right]^2 - \left[\frac{2\pi}{2b} \right]^2 = \left[\frac{2\pi\nu}{c} \right]^2 - \left[\frac{\pi}{b} \right]^2 = \left[\frac{2\pi}{c} \right]^2 (\nu^2 - \nu_c^2). \quad (1)$$

If the condition $\lambda_{\text{vac}} > 2b$ holds for the vacuum wavelength, the wave vector k is imaginary which is the "undersized" waveguide situation. The threshold $2b$ for λ_{vac} or the corresponding frequency value ν_c is known as the cutoff condition.

Another point of view emerged with the development of quantum mechanics. Within this description, a particle with a certain kinetic energy E can tunnel through a potential barrier of value $U > E$. This behavior is described by Schrödinger's equation and is the equation of the Helmholtz equivalent for a matter wave. There is, for some cases, a mathematical equivalence of guided electromagnetic waves and of matter waves in quantum mechanics. Quite recently, this has been pointed out again and studied both theoretically and experimentally.^{3,4} Martin and Landauer have demonstrated that one-dimensional particle tunneling is in direct analogy with electromagnetic pulse delay in a wave guide below a cutoff frequency.³ Thus, the undersized waveguide may be regarded as a one-dimensional (1D) tunneling barrier

for a quantum-mechanical particle as illustrated in Fig. 1. The barrier width is the length of the waveguide, the barrier height (potential U) is the $h\nu_c$ threshold at the cutoff frequency, and the measuring frequency represents the corresponding particle energy $E = h\nu$, where h is Planck's constant.

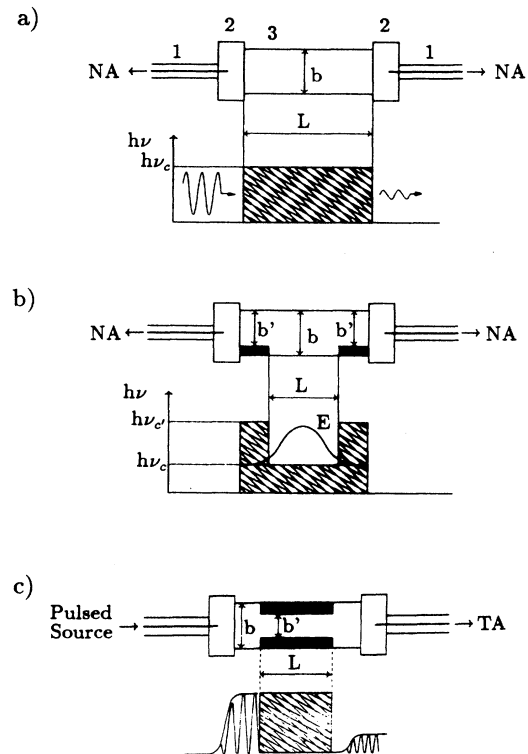


FIG. 1. (a) Experimental setup with coaxial lines (1) and transitions (2) to a rectangular waveguide section (3) of dimension b (22.86 mm) and of length L operated below cutoff corresponding to a photon potential barrier. (b) Setup for the double-barrier experiment with two barrier sections of dimensions b' (18.75 mm) operated below cutoff whereas the waveguide of length L was above the cutoff frequency. (c) Setup for the time-domain measurements ($b' = 15.8$ mm).

The debate over the tunneling process and its dynamics is still ongoing; it began some 60 years ago.^{3,5,6} Recently, the development of several tunneling devices such as, e.g., the tunneling microscope and semiconductor tunneling structures, has brought new urgency to the problem. Theoretical and experimental studies have concentrated on the question "How much time does tunneling take?"⁵

In this paper we present experimental data of barrier properties of photon ensembles in undersized waveguides. Such experiments are easier to realize than corresponding experiments on tunneling particles, as for instance with electrons. Rectangular waveguides (*X* band, cross section $10.16 \times 22.86 \text{ mm}^2$) were used, either below their cutoff frequency of 6.56 GHz [Fig. 1(a)] or by a further reduction of the related width of 22.86 mm within certain sections to yield higher cutoff frequencies [Fig. 1(b) by fitting metal plates into the *X*-band waveguide, Fig. 1(c) by the insertion of Ku-band waveguides with a cross section of $7.90 \times 15.80 \text{ mm}^2$]. The microwave experiments in the frequency domain have been performed with a HP8510B network analyzer (NA) system whereas in the time domain a HP70820 transition-analyzer system (TA) was used.

An experiment was performed to determine the dispersion relation *inside* the barrier region [Fig. 1(a)]. The scattering behavior of the coaxial cable-waveguide transitions depends on the electromagnetic boundary conditions and could, in principle, be determined, e.g., by an elaborate numerical field analysis or by special measurement procedures. However, this behavior is dependent on the special 3D transition geometries and is not comparable to that of the simple 1D boundary conditions of the potential-barrier problem. So it has been eliminated by measuring the transmission coefficient of tunneling sections with different lengths L . If appropriate conditions for L and the frequency range below cutoff are chosen, the attenuation will be too high for a significant influence of multiple reflections between the transitions. So the transmission coefficient is simply the product of the section response e^{ikL} and a transition-dependent, but length-independent, factor. In that case the dispersion relation is directly obtained from the quotient $e^{ik\Delta L}$ of two transmission coefficients of sections with length difference ΔL . In Fig. 2 the measured phase shift (i.e., the argument of $e^{ik\Delta L}$) and the attenuation of intensity (i.e., $|e^{2ik\Delta L}|$) for two such ΔL ratios (i.e., three barrier lengths have been measured) are shown as a function of frequency. The attenuation fulfills the theoretical values as predicted by the eigenvalue Eq. (1) for the Helmholtz wave equation. Measuring the phase shift it was found to be independent of L and frequency, i.e., barrier length and wave energy. Consequently the phase shift takes place at the transitions to the cutoff sections; inside the barrier it is zero. (Only the phase shift induced from the transition region is frequency dependent for opaque barriers with $|ikL| \gg 1$ as studied here.¹⁰) Already the shortest section length used for this evaluation had an attenuation of about 40 dB at the lowest frequency. Though a high-quality line-reflect-line calibration was performed at the coaxial port interface of the transitions,⁷ the additional lengths ΔL lowered the absolute transmit-

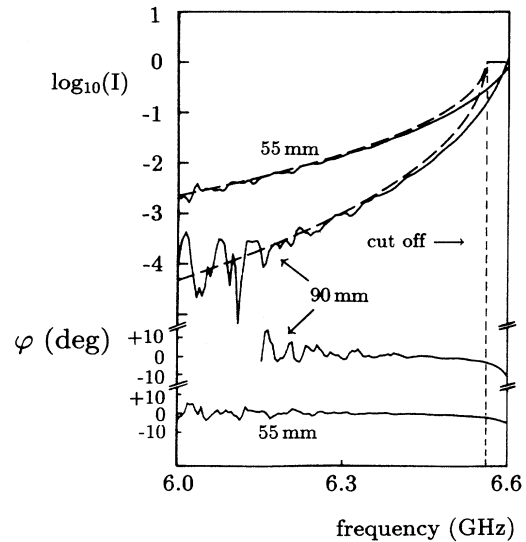


FIG. 2. Intensity attenuation I and phase shift φ of the transmitted wave for two differences in barrier length, $\Delta L = 55$ and 90 mm vs frequency. The response of the inner barrier region only is displayed; transition effects of the barrier boundaries have been eliminated as explained in the text. The dashed curves of intensity are theoretical values calculated from the eigenvalue Eq. (1).

ted levels down to the limits where the accuracy of the numerical aperture (NA) rapidly diminishes (therefore in Fig. 2 the phase of the longer section has been omitted below 6.15 GHz).

From inspection of Fig. 2 it is evident that above 6.4 GHz deviations from the "ideal" waveguide behavior [Eq. (1)] become important. Since the waveguide walls have losses there is no precise cutoff frequency and k has a real part already below the theoretical cutoff. Also multiple reflections and thus transition effects become important because of the lower attenuation. This behavior was additionally checked using three different types of coax-waveguide transitions which confirmed the results below 6.4 GHz and showed differently above so that real "subcutoff" conditions are ensured only 200 MHz or more below the theoretical cutoff.

With a double-barrier setup as sketched in Fig. 1(b) we have studied resonant tunneling. Waveguides (*X* band) with dimension $b = 22.86 \text{ mm}$ of different lengths L were placed between two short narrowed ones (40-mm length each). Thus for frequencies between the cutoff value of the large waveguide ν_c (6.56 GHz) and that of the barriers $\nu_{c'}$ (8.0 GHz) a cavity of length L with oscillatory eigenvalues $L = n\lambda/2$ is realized ($n = 1, 2, 3, \dots$). Its total response, including the barrier transitions, was measured. The influence of the coaxial cable-waveguide transitions was eliminated with a waveguide thru-reflect-line calibration procedure.⁷ The transmission intensity is displayed in Fig. 3 for two lengths. Pronounced transmission peaks up to 30 dB were observed; the peaks correspond to the cavity resonance frequencies.

The transmission peaks show two interesting features:

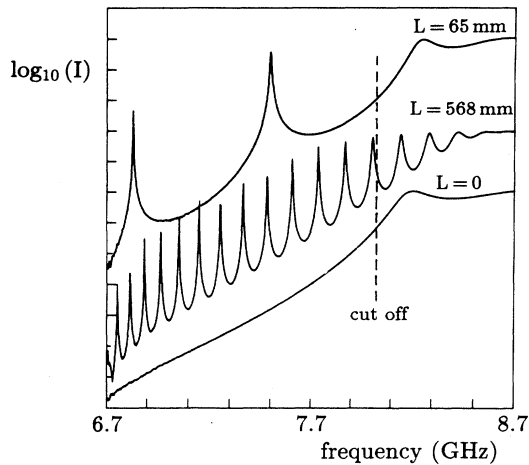


FIG. 3. Intensity attenuation I (one unit being an order of magnitude) of the transmission through the double-barrier quantum well. The curves have been shifted against each other. The transmission resonances are clearly seen for the two barrier distances L in comparison to a single barrier formed by zero distance. In consequence of the dispersion relation Eq. (1) the transmission peaks are not equidistant. Note that the experimental cutoff frequency is always observed above the theoretical value. This is a consequence of the strong dispersion approaching the cutoff value from higher frequencies, including the waveguide losses (Ref. 2), see also Fig. 2.

first, the resonant wavelengths are always significantly longer than those calculated with the geometrical length L . Obviously the standing waves penetrate to some extent into the barriers as indicated in the sketch of Fig. 1(b). For instance, at the resonator length $L = 65$ mm the lowest resonance frequency is expected for infinite barrier height at 6.947 GHz; however, it is observed at 6.823 GHz, and the second one is expected at 8.03 GHz and measured at only 7.49 GHz. This result is analogous with the quantum-mechanical eigenfrequencies in a potential well of finite depth. Second, the linewidth increases markedly with frequency approaching the cutoff value, i.e., the barrier height. The resonances' Q values ($\nu/\Delta\nu$ (center frequency divided by the width at half the maximal intensity)) correspond classically to the decay time τ of the stored energy $\tau = Q/2\pi\nu$. This resonant-state lifetime is usually assumed to represent a time scale for the resonant electron tunneling process.^{5,8,9} The decay time of the resonant states versus photon frequency is shown in Fig. 4. The two broken lines indicate the cutoff frequencies of the barriers and of the resonator waveguide, respectively [see Fig. 1(b)]. The decay time τ saturates approaching the lower cutoff value ν_c presumably in consequence of the rapidly increasing attenuation of the resonator waveguide at these frequencies. A corresponding time τ which was often assumed to represent a tunneling time has been calculated by the relation $\tau \approx (L/v)e^{-2ikl}$, where L is the resonator length, v the group velocity in the cavity, l is the barrier length, and k is the purely imaginary wave vector of the barriers.⁹ The deviations between our experiment and such a calculation

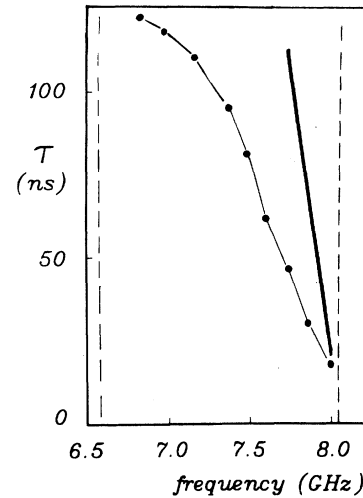


FIG. 4. Resonant-state decay time ($\tau = 1/2\pi\Delta\nu$) vs frequency of the double-barrier experiment with $L = 568$ mm. The data are taken from Fig. 3. Values near the cutoff regions were omitted; see discussion of Fig. 2. The two dashed lines correspond to the cutoff frequencies ν_c' and ν_c , the thick solid line represents theoretical values calculated by the formula given in the text. (Measured points have been connected by a line to guide the eye; the calculated thick line is only representative for resonance transitions.)

(solid line in Fig. 4 according to the above formula) diminish with frequency. The discrepancy may result from waveguide losses which limit the Q value of the resonance eventually.

With a setup as sketched in Fig. 1(c) direct signal delay-time measurements for a single barrier, including its transitions, were performed with the TA system in the time-domain mode. The narrowed waveguide regions were realized by the insertion of smaller waveguides (Ku band, cross section 7.90×15.80 mm², cutoff frequency 9.49 GHz). By switching the carrier frequency on and off (pulse width 1 μ s, pulse repetition frequency 10 kHz), an amplitude-modulated signal is produced [see Fig. 1(c)]. Fourier analysis gives an infinite spectrum of frequencies distributed around the carrier frequency. The waveguide below cutoff transmits higher-frequency components due to Eq. (1) (see also Fig. 2), eventually above cutoff the attenuation becomes negligible. Since only the tunneling times through the barrier below cutoff were of interest conditions had to be chosen so that the transmitted signal was composed essentially of frequency components below cutoff (tunneling regime). This can be easily checked: a considerable amount of energy in frequencies around or above the cutoff has a low attenuation. Consequently there will be multiple reflections between the transitions which cause a ripple of the signal's envelope in the time domain before reaching the stationary state.

In Fig. 5(a) the measured pulse envelope is displayed for the reference pulse and three different barriers lengths (carrier frequency 8.5 GHz, 400 measurement points with 50-ps distance, 62.5-kHz digital noise filter and subsampling mode, trace averaging of 5, 10, 20, and 1024, re-

spectively). The successive shifts of the noise floor level from about -40 dB to less than -65 dB is caused by a system-inherent limitation of the transition-analyzer system. Its dynamic range is limited to about 40 dB when measuring transient times less than 50 ns which is the case here. Consequently the noise floor of such fast transients will be raised above the input sensitivity level of the transition analyzer if the largest value of the transient is more than 40 dB above that sensitivity. This effect is obvious inspecting Fig. 5(a). Note that this reduces only the accuracy of the lower transient level which is the noise floor—the upper values are not altered. The stationary values of transmission which are nearly reached after 20 ns correspond to within ± 1 dB to the theoretical attenuation values calculated from Eq. (1) and the corresponding barrier-section lengths of 40 and 60 mm. This also indicates that under these special experimental conditions the transition effects from the larger waveguide to the cutoff section can be neglected compared to the section response itself (see below).

At the length $L = 120$ mm a multiple reflecting ripple

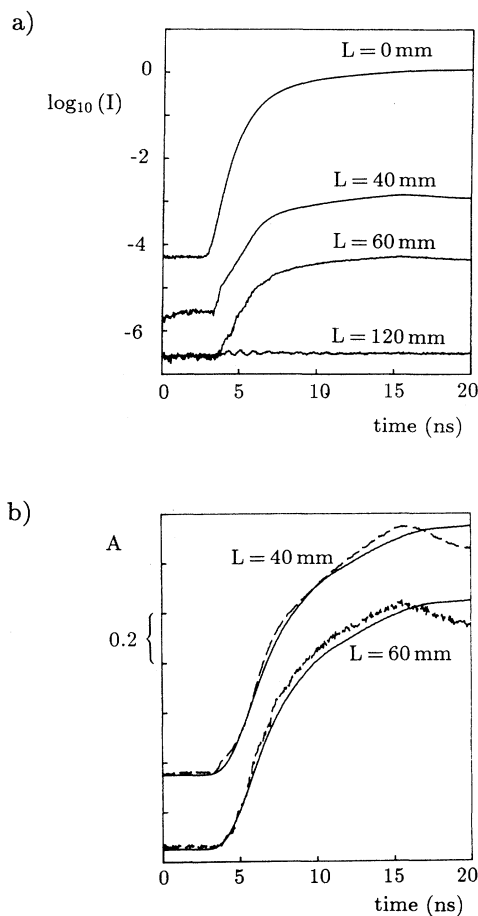


FIG. 5. (a) Intensity attenuation I vs time for the rising edges of the reference ($L = 0$ mm) and transit pulses for three barriers (b) normalized, linear amplitude A vs time for two barrier lengths (dashed lines), and the reference (solid lines). More details are given in the text.

is seen at the beginning of the pulse. This structure is generated essentially from frequency components in the range of cutoff or above. The calculated transmission intensity of the carrier frequency is about 10^{-9} for $L = 120$ mm and thus not resolvable reaching the stationary state. Here the above-mentioned problem occurs which must be accounted for in doing such experiments on the tunneling times through opaque barriers (opaque is a sloppy expression for “sufficiently” wide and high barriers; here it is used as a synonym for the condition that multiple reflections within the barrier do not alter the transmission properties more than the range of the measurement accuracy): The carrier frequency as well as the pulse envelope should be chosen such that the measured transition time response is again determined by a frequency distribution having its main intensity at least 200 MHz below cutoff. Since the pulse form was fixed by the source only the carrier frequency could be altered. Measurements were made at different barrier lengths (range 40 to 180 mm) and carrier frequencies at 8.5, 8.8, and 9.1 GHz. At 8.8 and 9.1 GHz, however, always a periodic ripple due to a higher-frequency contribution could be seen, making a single-passage-time determination more difficult or impossible. So 8.5 GHz was chosen where this effect was acceptable with the two shown barrier lengths of $L = 40$ and 60 mm but occurred again with the length of 120 mm.

In Fig. 5(b) the amplitude time response at 8.5-GHz carrier frequency is displayed on a linear, normalized scale (each curve normalized to the same amplitude of 1) for the two barrier lengths in comparison to the reference pulse. The drop of the barrier response above 15 ns is caused by the reflection from the barrier back to the source and again back to the barrier input. It was identified by shorter lengths of the feeding coaxial line. They shifted this drop by exactly twice the altered delay length of the cable. At this very point it should be noted that there is no additional inaccuracy to the chosen 50-ps point-to-point distance resolution of the time base due to jitter or other effects: the used transition-analyzer system derives the timing for both the pulsed source, including the pulse generator as well as the carrier frequency, and for the trigger circuitry of the receiver from the same time basis (phase-locked-loop coupling of all of them to a 10-MHz crystal oven with a specified stability of better than 10^{-9} per day; a drift of the reference pulse measurement of Fig. 5 was not resolvable after a 2-day period).

Figure 5(b) seems to indicate that there is a noncausal connection of the barrier transit compared to the incident pulse up to 15 ns. However, the filter function of the cutoff section shifts the spectral intensity to higher frequencies (including the above-mentioned cutoff components) and thus alters the shape of the response. In the extreme the transmitted signal would only contain the high-frequency components of the reference signal which have low amplitudes but are not attenuated in the cutoff section; if this level is normalized and thus amplified to the level of the reference signal, high-frequency amplitudes are generated which are only negligibly present in the reference signal. This happens in the normalization procedure. Under the present conditions this effect is

very small but causes the alleged noncausality of Fig. 5(b). This makes a time-delay measurement only between the rising edges of the pulse difficult.

On the other hand, the deformation of the rising edges behind the two barriers of different length is very low. Up to the 15-ns range the edge shapes are nearly equal compared to each other as well as to the reference. Consequently transit delay times for such opaque barriers are well defined, also for the maximum or the center of gravity of wave packets. Corresponding measurements could be performed if the technical problems of generating adequate pulses can be solved (they must have negligible intensities of frequencies above cutoff and must be short enough, so that delay effects of the whole pulse envelope can be resolved). Due to the present results a lower limit for the traversal velocity can be estimated. The largest time error will be the largest time difference between barrier and reference response due to the different shaping of the edge. This value is about ± 1.5 ns for the barrier of 60-mm length. A corresponding lowest value of the traversal velocity is about 0.2 times c , the vacuum velocity of light. The experimental result includes also superluminal barrier crossing since no lower limit for the time difference between barrier and reference response could be measured.^{3,10}

In summary, we have pointed out the experimental and interpretational problems of photon tunneling. We have

given a comprehensive experimental description of the stationary transmission properties of photonic barriers both through a single barrier as well as a resonant structure realized by two barriers. Time-domain measurements have given the first traversal delay properties for an opaque barrier. The deformation of the signals after barrier traversal is low. Incident and transmitted wave packets are comparable with respect to their maximum or center of gravity so that delay-time measurements are well defined. In this paper a lower limit for the traversal velocity of $0.2c$ was derived. It has also been shown that resonant-state decay times of a double-barrier configuration are more than one order of magnitude larger than the nonresonant barrier traversal time ≤ 1.5 ns. Most fascinating is the aspect that the feasibility of photon delay measurements has now become possible for opaque-barrier conditions.

We gratefully acknowledge discussions with A. Kirchner, W. Klein, D. Kreimer, P. Mittelstaedt, R. Pelster, and H. Spieker and essential technical support by S. Mäcker, and by H. Aichmann, M. Hechler, and W. Strasser at Hewlett-Packard, as well as financial support by the Verein der Freunde und Förderer der Universität zu Köln.

¹L. Brillouin, *Wave Propagation and Group Velocity* (Academic, New York, 1960); L. Brillouin, *Wave Propagation in Periodic Structures* (Dover, New York, 1953).

²J. D. Jackson, *Classical Electrodynamics* (Wiley, New York, 1974).

³T. Martin and R. Landauer, *Phys. Rev.* **45**, 2611 (1992).

⁴A. Ranfagni, D. Mugnai, P. Fabeni, and G. P. Pazzi, *Appl. Phys. Lett.* **58**, 774 (1991).

⁵E. H. Hauge and J. A. Støvneng, *Rev. Mod. Phys.* **61**, 917 (1989).

⁶V. S. Olkhovsky and E. Recami, *Phys. Rep.* **214**, 339 (1992).

⁷A generalized theory on the important topic of NA calibration procedures can be found in H.-J. Eul and B. Schiek, *IEEE Trans. Microwave Theory Tech.* **39**, 724 (1991).

⁸M. Tsuchiya, T. Matsusue, and H. Sakak, *Phys. Rev. Lett.* **59**, 2356 (1987).

⁹J. A. Støvneng and E. H. Hauge, *Phys. Rev. B* **44**, 13 582 (1991).

¹⁰A. Enders and G. Nimtz, *J. Phys. I (France)* **2**, 1693 (1992).